International Journal of Heat and Technology
Vol. 44, No. 1, February, 2026, pp. 153-166
Journal homepage: http://iieta.org/journals/ijht

Second-Law-Constrained Model Decomposition and Real-Time Simulation of Electrical–Thermal Coupling Systems in Nuclear Power Plants

Song Yang*, Lichao Tian

Huaneng Hainan Changjiang Nuclear Power Co., Ltd., Changjiang 572700, China

Corresponding Author Email: yangsong@hcnpc.chng.com.cn

https://doi.org/10.18280/ijht.440113

Received: 10 October 2025
Revised: 9 February 2026
Accepted: 22 February 2026
Available online: 28 February 2026

Keywords:
second law of thermodynamics, entropy production rate spectrum, maximum entropy production principle, electrical–thermal coupling, dynamic model decomposition, real-time simulation, nuclear power plant, non-equilibrium thermodynamics

ABSTRACT

As for high- and medium-voltage electrical–thermal coupling systems in nuclear power plants, conventional real-time simulation employs the second law of thermodynamics only as a posteriori validation criterion, failing to guarantee thermodynamic consistency and numerical stability during simulation. This study elevates the second law of thermodynamics from a constraint to the first-principles foundation and organizing principle of the real-time simulation framework, establishing a non-equilibrium thermodynamics-driven theoretical architecture for electrical–thermal coupled real-time simulation. The proposed dynamic model decomposition method based on entropy production rate spectrum analysis enables adaptive and precise identification of dynamic boundary layers within the coupled system. Furthermore, the developed entropy-preserving data interaction mechanism grounded in the maximum entropy production principle ensures physically compliant transfer of energy and entropy between electrical and thermal submodels. The proposed nonlinear variable-step solution strategy oriented toward thermodynamic time allows the relaxation characteristics of the system to be consistently matched with real-time computational requirements. The method enables a unified characterization of numerical stability and thermodynamic stability, thereby resolving the stiffness challenges inherent in strongly coupled multiscale systems from a fundamental physical perspective. Validation under representative operating scenarios—including steady-state operation of the nuclear power plant, grid short-circuit disturbances, and abrupt steam load variations—demonstrates superior physical self-consistency, numerical robustness, and real-time computational performance. This work establishes a novel paradigm for the application of non-equilibrium thermodynamics in the real-time simulation of complex energy systems and provides foundational theoretical and technical support for safety analysis and control validation of electrical–thermal coupling systems in nuclear power plants.

1. INTRODUCTION

High- and medium-voltage electrical–thermal coupling systems in nuclear power plants encompass multiple interacting physical processes, including electromagnetic transients, energy transfer, and thermodynamic dissipation [1, 2]. These systems exhibit pronounced multiscale characteristics, strong nonlinear interactions, and severe numerical stiffness. Real-time simulation serves as a core technological instrument for safety assessment, fault mechanism analysis, and control strategy validation in nuclear power plant systems [3-5], directly determining operational reliability and the effectiveness of disturbance mitigation. Current research on real-time simulation of complex energy systems has largely concentrated on numerical algorithm optimization [6, 7] and computational architecture enhancement [8, 9]. However, the fundamental physical constraints imposed by irreversible processes are frequently overlooked. As a consequence, deviations may arise between the simulation result and actual physical evolution. Non-equilibrium thermodynamics, as the foundational theory describing irreversible energy conversion and dissipation processes [10, 11], enables quantitative characterization of entropy variation, entropy production, and the evolution of energy quality within complex systems, offering a fundamental physical basis for the modeling and simulation of complex coupled systems. Reconstruction of the simulation paradigm around non-equilibrium thermodynamic principles not only enhances physical fidelity and intrinsic stability but also promotes a transition from mathematically driven simulation frameworks to physics-driven methodologies. Such a transformation is of substantial scientific significance and engineering value for the accurate simulation and safe operation of electrical–thermal coupling systems in nuclear power plants.

Existing studies on real-time simulation of electrical–thermal coupling systems predominantly rely on mathematical stiffness analysis as the principal criterion for model decomposition [12]. Decomposition boundaries are typically aligned with fixed physical interfaces [13], limiting

adaptability to dynamically evolving disturbances. Boundary data exchange between subsystems often lacks unified physical constraints, which may induce distortion in energy transfer and thermodynamic inconsistency [14, 15]. Furthermore, the selection of simulation time steps is generally governed by numerical error control strategies, rather than by the intrinsic thermodynamic evolution of the system. Consequently, coordinated optimization between real-time performance and computational fidelity remains difficult to achieve [16]. Under such conditions, thermodynamic consistency cannot be rigorously guaranteed throughout the simulation process. When subjected to strong disturbances or far-from-equilibrium operating regimes, numerical instability and simulation failure may readily occur.

Four fundamental scientific challenges remain unresolved within existing real-time simulation frameworks. First, numerical stability in simulation and thermodynamic stability of the system are treated as independent constructs, and no unified mathematical representation or constraint framework has been established to couple them coherently [17]. Second, model decomposition of electrical–thermal coupling systems is conducted primarily on the basis of mathematical criteria, while quantitative decision metrics derived from non-equilibrium thermodynamics are largely absent [18]. Third, data exchange across heterogeneous subsystems does not systematically adhere to the physical laws governing irreversible processes, thereby preventing rigorous enforcement of entropy balance and energy transfer [19, 20]. Fourth, the simulation time scale is not aligned with the intrinsic thermodynamic relaxation characteristics of the system, making it difficult to satisfy the demands of refined simulation under far-from-equilibrium disturbances [21].

To address these limitations, the conventional paradigm in which the second law of thermodynamics is treated merely as a posteriori evaluation criterion is transcended. Instead, it is elevated to the status of a first-principles foundation and central organizing logic for real-time simulation. A non-equilibrium thermodynamics-driven real-time simulation methodology for high- and medium-voltage electrical–thermal coupling systems in nuclear power plants is thereby established. The principal innovations are manifested in three aspects. First, a dynamic model decomposition method based on entropy production rate spectrum analysis is developed, enabling adaptive identification of coupling boundaries and domain-partitioned solution of subsystem models. Second, an entropy-preserving data interaction mechanism grounded in the maximum entropy production principle is proposed to ensure physical consistency in energy and entropy transfer across heterogeneous subsystems. Third, a nonlinear variable-step solution strategy oriented toward thermodynamic time is designed, allowing dynamic matching between simulation step size and the intrinsic thermodynamic relaxation characteristics of the system. Through these developments, numerical stability and thermodynamic stability are unified at the physical level, and the stiffness challenges inherent in strongly coupled multiscale systems are fundamentally mitigated.

The remainder of this study is organized below. In Section 2, the second law of thermodynamics is reformulated as the first-principles foundation of the simulation framework, and a thermodynamically constrained manifold together with a unified stability characterization framework is constructed. Section 3 introduces the dynamic model decomposition method based on entropy production rate spectrum analysis, with explicit decomposition criteria and boundary identification algorithms. Section 4 establishes the entropy-preserving data interaction mechanism derived from the maximum entropy production principle and formulates the cross-domain subsystem interaction protocol. Section 5 presents the nonlinear variable-step solution strategy based on thermodynamic time and develops a collaborative simulation architecture for heterogeneous platforms. Section 6 provides validation under representative nuclear power plant operating conditions, and comparative analyses are conducted to demonstrate the performance advantages of the proposed methodology. Section 7 discusses the theoretical contributions, practical implications, and potential extensions. Section 8 concludes with a synthesis of the principal findings and core conclusions.

2. PARADIGM RECONSTRUCTION OF REAL-TIME SIMULATION

Conventional simulation paradigms are centered on mathematical stiffness analysis for system decoupling and model decomposition. Such an approach, however, does not fundamentally align with the intrinsic irreversibility of high- and medium-voltage electrical–thermal coupling systems in nuclear power plants. Within this framework, the second law of thermodynamics is treated merely as a posteriori validation criterion, whereby the non-negativity of entropy production is examined only after completion of the simulation to assess result plausibility. Consequently, no active constraint is enforced during the simulation evolution itself. As a result, numerical stability in computation and thermodynamic stability of the system remain conceptually and mathematically disconnected. This separation allows the simulation trajectory to deviate from the underlying physical principles. Under far-from-equilibrium operating conditions in particular, distortions in energy transfer, violations of entropy balance, and inconsistencies in entropy production may arise. Such deviations ultimately manifest as numerical instability or even simulation failure. This intrinsic limitation substantially restricts the physical fidelity and robustness of traditional methodologies and renders them inadequate for high-precision real-time simulation of complex coupled systems. Figure 1 illustrates a schematic comparison between the conventional simulation paradigm and the thermodynamics-driven simulation paradigm proposed herein.

A thermodynamic first-principles framework for real-time simulation of electrical–thermal coupling systems is reconstructed. The physical essence of model decomposition is explicitly reinterpreted as an information-theoretic mapping of irreversible processes, rather than as a purely mathematical forced partition. On the basis of the axioms of non-equilibrium thermodynamics, and starting from the non-negativity of entropy production, it is theoretically established that the second law of thermodynamics defines the physical admissibility condition for simulation algorithm stability. Let the system state vector be denoted by x, and let the numerical evolution operator be represented by F. For any physically admissible simulation algorithm, the global entropy production rate induced by $F(x)$ must satisfy $\dot{S}_{gen}\geq 0$. If there exists an evolution step for which $\dot{S}_{gen}<0$, the corresponding numerical evolution necessarily violates the physical law of irreversibility and must therefore be regarded as physically inadmissible. On this basis, a thermodynamically constrained

manifold is constructed using a Lyapunov function formulation. The total entropy production functional of the system is defined as $\dot{S}_{gen}=\int_V \sigma(x,t)dV$, where $\sigma(x,t)$ denotes the local entropy production rate at spatial position x and time t, and V represents the spatial domain of the system. The Lyapunov function is selected as $V(x,t)=\dot{S}_{gen}$. By enforcing $\dot{V}(x,t)\geq 0$, thermodynamic consistency of the simulation evolution is guaranteed. The thermodynamically constrained manifold thus becomes the physical boundary of the feasible numerical solution space. The simulation paradigm is transformed from a mathematics-driven framework to a physics-driven formulation. Figure 2 illustrates the schematic representation of the thermodynamically constrained manifold and the feasible domain of numerical solutions.

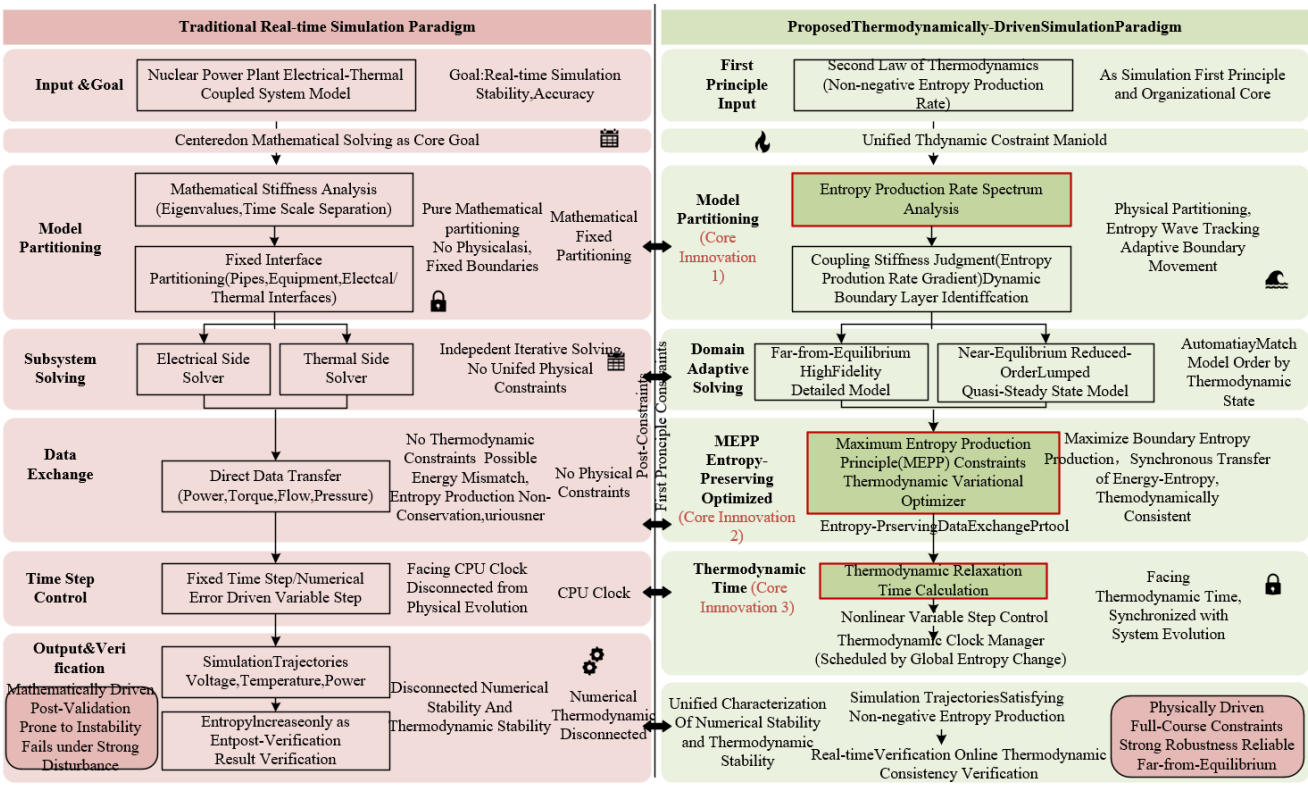

Figure 1. Schematic comparison between the conventional simulation paradigm and the thermodynamics-driven simulation paradigm

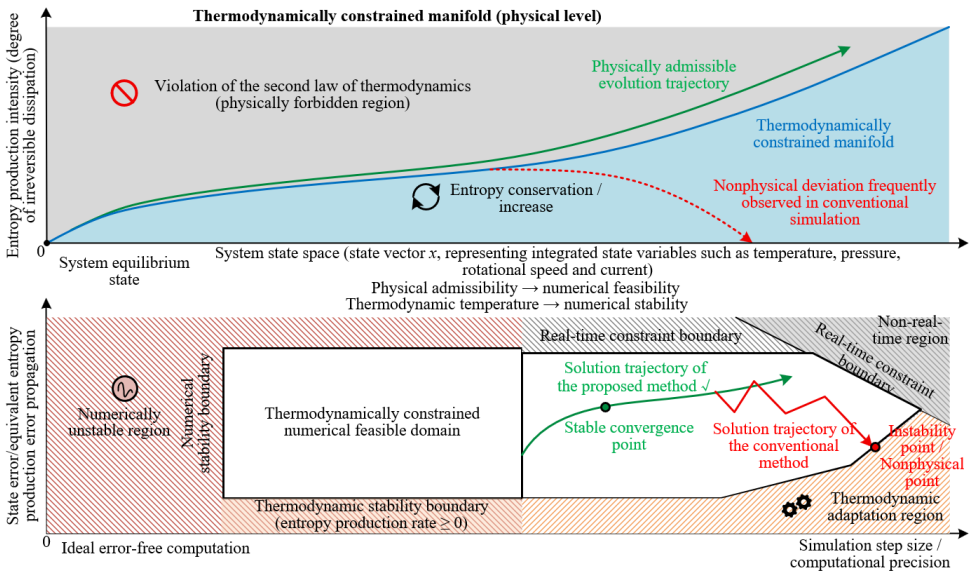

Figure 2. Schematic representation of the thermodynamically constrained manifold and the feasible domain of numerical solutions

A unified mathematical formulation of numerical stability and thermodynamic stability is established, thereby overcoming the conventional separation between these two concepts. An entropy-production-equivalent representation of truncation and round-off errors is introduced. In numerical computation, truncation error Δx_{trunc} and round-off error Δx_{round} induce an associated energy deviation ΔE_{err}. This deviation is transformed into an equivalent entropy production

term σ_{err}, defined as $\sigma_{err}=\Delta E_{err}/T_{ref}$, where T_{ref} denotes a characteristic reference temperature of the system. Through this transformation, the accumulation of numerical errors is quantitatively mapped onto an equivalent entropy production rate. On the basis of the global entropy production non-negativity criterion, the feasible domain of numerical solutions is redefined as $\dot{S}_{gen}+\sigma_{err}\geq 0$. Under this condition, numerical stability requirements are embedded directly within the thermodynamically constrained framework. The permissible range of numerical error is thus explicitly bounded: the superposition of the equivalent entropy production and the system's intrinsic entropy production must remain non-negative at all times. Through this formulation, cumulative numerical error and the entropy-increasing tendency are regulated in a coordinated manner. In this way, the longstanding conceptual separation between numerical stability and thermodynamic stability is resolved at the physical level. This unified representation provides a coherent theoretical foundation and constraint criterion for subsequent dynamic model decomposition, cross-domain data interaction, and real-time solution strategies.

3. DYNAMIC MODEL DECOMPOSITION VIA ENTROPY PRODUCTION RATE SPECTRUM ANALYSIS

For the high- and medium-voltage electrical–thermal coupling system of a nuclear power plant, a distributed entropy production rate model is established. Analytical expressions for the local entropy production rate of key components are explicitly formulated, providing a quantitative foundation for constructing the entropy production rate spectrum. For the reactor core, the local entropy production rate is dominated by the irreversibility associated with nuclear heat release and convective heat transfer to the coolant. The corresponding analytical expression is written as:

$$\sigma_{core}=\frac{q''}{T_{fuel}}-\frac{q''}{T_{cool}} \tag{1}$$

where, q'' denotes the heat flux at the fuel rod surface, T_{fuel} represents the fuel cladding temperature, and T_{cool} is the bulk coolant temperature. For the steam generator, entropy production arises from both heat transfer and flow dissipation. It is expressed as:

$$\sigma_{sg}=\frac{Q}{T_1}-\frac{Q}{T_2}+\frac{\Delta P_{\dot{m}}}{T_{avg}} \tag{2}$$

where, Q denotes the heat transfer rate, T_1 and T_2 are the average temperatures of the primary and secondary working fluids, respectively, ΔP represents the pressure drop, $\dot{m}$ is the mass flow rate, and T_{avg} is the average fluid temperature. For the high- and medium-pressure turbine stages, entropy production is governed by the irreversibility of steam expansion, i.e.,

$$\sigma_{turb}=\dot{m}(s_1-s_2)-\frac{\dot{W}_{act}}{T_{turb}} \tag{3}$$

where, s_1 and s_2 denote the specific entropy at the turbine inlet and outlet, respectively, $\dot{W}_{act}$ denotes the actual output power, and T_{turb} represents the average operating temperature of the steam turbine. The entropy production rate of the generator corresponds to electromagnetic and mechanical losses, and is expressed as $\sigma_{gen}=P_{loss}/T_{gen}$, where T_{gen} is the average stator temperature of the generator. The entire system is treated as a distributed parameter system. The control volumes of each component are discretized using the finite volume method, and the spatiotemporal evolution of the entropy production rate is obtained by solving the following governing equation:

$$\frac{\partial \sigma}{\partial t}+\nabla\cdot(\sigma u)=\dot{\sigma}_{source} \tag{4}$$

where, u denotes the working fluid velocity and $\dot{\sigma}_{source}$ represents the entropy production source term. Through this formulation, the entropy production rate spectrum of the entire system is constructed, enabling quantitative characterization of irreversible dissipation intensity across different regions. Figure 3 presents a schematic of the system entropy production rate spectrum and the principle of dynamic boundary layer identification.

An original quantitative criterion for coupling stiffness based on the magnitude of the entropy production rate gradient is proposed, thereby replacing conventional eigenvalue-based mathematical stiffness diagnostics with a physically grounded measure. The coupling stiffness K is defined as the magnitude of the spatial gradient of the local entropy production rate:

$$K=\|\nabla\sigma\|=\sqrt{\left(\frac{\partial\sigma}{\partial x}\right)^2+\left(\frac{\partial\sigma}{\partial y}\right)^2+\left(\frac{\partial\sigma}{\partial z}\right)^2} \tag{5}$$

where, σ denotes the local entropy production rate, and x, y, z represent the spatial coordinates. The core innovation of this criterion lies in the direct linkage established between coupling stiffness and irreversible dissipation. A smaller value of K indicates a relatively smooth spatial distribution of entropy production, weaker interaction among physical processes, and proximity to local thermodynamic equilibrium. Conversely, a larger value of K signifies pronounced spatial variation in entropy production, intensified irreversibility in energy conversion between electrical and thermal domains, and strong coupling behavior. Through this formulation, the decision basis for model decomposition is elevated from a purely mathematical level to a physical level. As a result, the partitioning result remains consistent with the intrinsic thermodynamic evolution of the system, thereby preventing the physical distortions that may arise from conventional mathematically enforced decomposition.

A dynamic boundary layer adaptive identification algorithm is further constructed. By combining threshold discrimination of coupling stiffness with entropy wavefront tracking, real-time dynamic updating of decomposition boundaries is achieved. The critical coupling stiffness threshold K_{cr} is determined by fitting steady-state operational data of the system, satisfying $K_{cr}=k\cdot\overline{K}_{steady}$, where k is a correction coefficient (typically within the range 1.2–1.5), and K_{steady} denotes the average coupling stiffness under steady-state conditions. Based on this criterion, the system state is classified into near-equilibrium regimes ($K\leq K_{cr}$) and far-from-equilibrium regimes ($K>K_{cr}$). When disturbances occur, regions exhibiting abrupt variation in entropy production propagate in the form of entropy waves. The propagation velocity of the entropy wavefront is defined as:

$$v_{wave}=\frac{\partial\sigma/\partial t}{\|\nabla\sigma\|} \tag{6}$$

The entropy wavefront position is tracked in real time by integrating the velocity:

$$r(t)=r_0+\int_0^t v_{wave}\,dt \tag{7}$$

where, r_0 denotes the initial disturbance location. At each simulation step, the global distribution of coupling stiffness is evaluated, and the entropy wavefront is identified as a dynamic boundary layer. In this manner, the decomposition boundary is adaptively updated in synchrony with disturbance propagation, ensuring that partition interfaces remain precisely aligned with regions of concentrated dissipation.

Based on the dynamically identified boundary layers, a rigorous domain-adaptive modeling rule is established to achieve coordinated optimization between simulation accuracy and computational efficiency. Within near-equilibrium regions, the system approaches local thermodynamic equilibrium, and thermodynamic forces and fluxes approximately satisfy the Onsager reciprocal relations. Reduced-order models are therefore employed. On the thermal side, a lumped-parameter model is adopted, and the entropy production rate is simplified as:

$$\sigma_{lump}=\frac{\sum \dot{Q}_i}{T_{avg}}-\frac{\sum \dot{W}_i}{T_{avg}} \tag{8}$$

On the electrical side, a quasi-steady-state model is employed. High-frequency electromagnetic transient components are neglected, and only the evolution of the fundamental frequency component is computed. Within far-from-equilibrium regions, nonlinear effects become significant, and the Onsager reciprocal relations are no longer applicable. High-fidelity models are therefore adopted. On the thermal side, a reduced computational fluid dynamics formulation is applied, in which the three-dimensional Navier–Stokes equations coupled with the energy equation are solved to obtain the spatial distribution of entropy production. On the electrical side, a full-order electromagnetic transient model is employed. The Park transformation equations are solved, and entropy production associated with electromagnetic losses is computed accordingly. The adaptive rule dynamically matches the thermodynamic state of the system with model complexity in real time. Under the global entropy production non-negativity constraint, computational efficiency is maximized, providing high-efficiency and high-precision model support for real-time simulation.

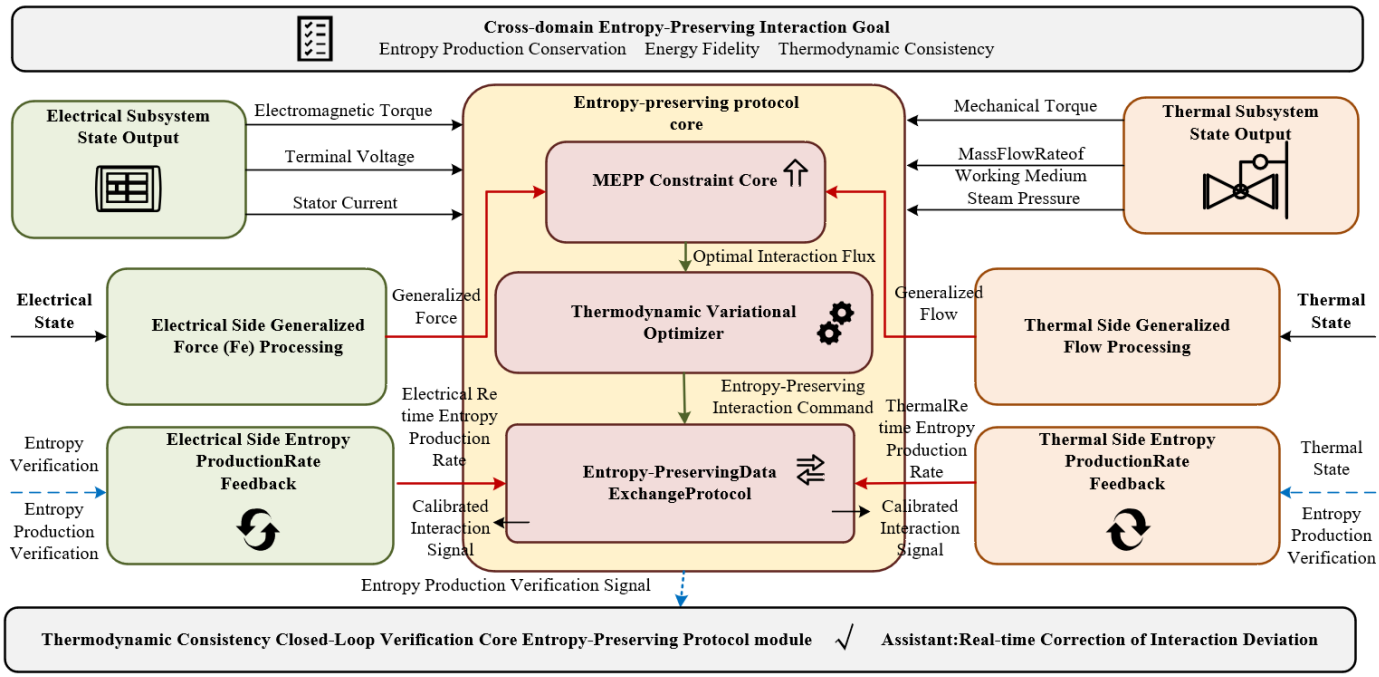

Figure 3. Architecture of the cross-domain entropy-preserving data interaction protocol based on the maximum entropy production principle

4. CROSS-DOMAIN ENTROPY-PRESERVING DATA INTERACTION MECHANISM

In conventional real-time simulation frameworks, boundary data exchange between electrical and thermal subsystems is performed primarily at the numerical level, without strict adherence to the physical laws governing irreversible energy conversion. As a consequence, thermodynamic inconsistencies may arise during cross-domain interaction, including loss of physical information, artificial energy injection, and violation of entropy balance. Such thermodynamic mismatch directly compromises the overall thermodynamic consistency of the coupled simulation system. The evolution of boundary energy flux and entropy flux may deviate from physical reality, and under strong coupling disturbances or far-from-equilibrium conditions, numerical oscillations may be amplified, ultimately leading to simulation instability. These deficiencies prevent conventional approaches from supporting high-fidelity real-time simulation of electrical–thermal coupling systems in nuclear power

plants.

To resolve this limitation, the maximum entropy production principle is adopted as the core physical criterion for cross-domain entropy-preserving data interaction. All energy and entropy exchanges occurring across dynamic boundaries are required to maximize the total entropy production rate, subject to system state constraints and energy conservation laws. Let $\dot{S}_{gen,e}$ and $\dot{S}_{gen,t}$ denote the entropy production rates of the electrical and thermal subsystems, respectively, and let $\dot{S}_{gen,b}$ represent the entropy production induced by boundary interaction. The total entropy production rate of the coupled system satisfies $\dot{S}_{gen}=\dot{S}_{gen,e}+\dot{S}_{gen,t}+\dot{S}_{gen,b}$. The total entropy production rate is treated as the optimization objective. The optimal boundary interaction flux is determined through the variational extremum condition $\delta S_{gen}=0$. Through this procedure, cross-domain interaction is aligned with the natural evolution trajectory of the non-equilibrium thermodynamic system, and thermodynamic mismatch is eliminated at its physical origin.

An entropy-preserving data exchange protocol tailored for electrical–thermal coupling systems is further constructed. A rigorous coupling relationship between generalized forces and generalized fluxes at the dynamic boundary is established. On the electrical side, generalized force variables—such as electromagnetic torque and terminal voltage—are denoted by F_e. On the thermal side, generalized flux variables—such as mechanical torque and working fluid mass flow rate—are denoted by J_t. The instantaneous exergy transfer rate across the boundary satisfies $\dot{E}_x = F_e \cdot J_t$. A quantitative constraint exists between the boundary entropy production rate and the exergy transfer rate:

$$\dot{S}_{gen,b}=\frac{\dot{E}_x}{T_b} \tag{9}$$

where, T_b denotes the characteristic dynamic boundary temperature. The proposed protocol strictly constrains both the form and numerical relationships of transmitted variables, ensuring that exergy transfer and entropy production evolve in a quantitatively matched manner. This ensures entropy production conservation throughout the entire cross-domain interaction process. Figure 3 illustrates the architecture of the cross-domain entropy-preserving data interaction protocol based on the maximum entropy production principle.

A thermodynamic variational optimizer is constructed to implement entropy-preserving interaction at the algorithmic level. Within each single real-time simulation cycle, variational optimization of the boundary constraints is completed. A Lagrange multiplier λ is introduced to construct the augmented objective function $L = \dot{S}_{gen}+\lambda(\dot{E}_x-F_e \cdot J_t)$. The optimal boundary interaction variables are obtained by solving the condition $\nabla L = 0$. The electrical subsystem executes sub-microsecond computation of generalized force variables using a field-programmable gate array (FPGA) parallel architecture. The thermal subsystem performs iterative computation of generalized flux variables using a multi-core central processing unit (CPU) parallel architecture. Both subsystems are synchronized using a unified thermodynamic clock. Within a single simulation time step, bidirectional variable exchange and variational optimization are completed, enabling coordinated interaction and numerical synchronization across heterogeneous FPGA and CPU platforms.

A real-time thermodynamic consistency verification method is further established to enable online quantitative assessment of boundary interaction validity. A thermodynamic consistency verification function is defined as $\Xi=\dot{S}_{gen}-\dot{S}_{gen,mepp}$, where $\dot{S}_{gen,mepp}$ denotes the theoretical entropy production rate that satisfies the maximum entropy production principle. A verification threshold Ξ_{th} is prescribed. When $\Xi \geq -\Xi_{th}$, the interaction process is considered thermodynamically consistent. When $\Xi < -\Xi_{th}$, automatic reconstruction of boundary variables and iterative optimization correction are triggered. Through this mechanism, interaction errors are detected and rectified in real time, thereby ensuring entropy production conservation and physical fidelity throughout the entire simulation process.

5. NONLINEAR VARIABLE-STEP REAL-TIME SOLUTION STRATEGY

Conventional real-time simulation strategies typically regulate the time step according to either the physical clock or numerical truncation error control. Such approaches are detached from the intrinsic thermodynamic evolution of the system and therefore fail to adapt to the state-dependent dynamics of electrical–thermal coupling systems in nuclear power plants. A fixed time step cannot simultaneously accommodate fine-resolution simulation under far-from-equilibrium conditions and high computational efficiency near equilibrium. Similarly, truncation-error-based variable-step strategies focus exclusively on numerical accuracy while neglecting entropy production evolution. As a consequence, the simulation time step may become mismatched with the system's thermodynamic relaxation characteristics, resulting either in excessive computational expenditure or insufficient physical fidelity. These limitations prevent conventional approaches from meeting the requirements of real-time simulation in complex coupled systems.

To address this deficiency, an original definition of thermodynamic relaxation time based on the local entropy production rate is introduced. This relaxation time quantitatively characterizes the intrinsic time scale over which the system evolves from a non-equilibrium state toward local thermodynamic equilibrium and is computed dynamically in real time. The thermodynamic relaxation time τ is defined as $\tau = C/k\sigma$, where C is a thermodynamic constant determined by working fluid properties and component structural parameters, k is a correction coefficient (typically within the range 0.8–1.0), and σ is the local entropy production rate obtained from real-time computation. This formulation establishes a direct physical linkage between relaxation time and irreversible dissipation intensity. When σ is large, the system is far from equilibrium, and the relaxation time τ becomes small, indicating rapid system evolution. Conversely, when τ increases, this corresponds to slower evolution dynamics. By solving for the spatial distribution of σ across all control volumes, the spatiotemporal distribution of thermodynamic relaxation time for the entire system is obtained, thereby providing a direct physical basis for time-step control.

A nonlinear step-size control law based on thermodynamic relaxation time is subsequently established to achieve dynamic matching between the simulation time step and the intrinsic thermodynamic evolution of the system. The time step h is nonlinearly correlated with the thermodynamic relaxation time τ, and the control law is expressed as $h=\alpha\tau$, where α is a step-

size adjustment coefficient selected adaptively according to simulation accuracy requirements (typically within the range 0.1–0.3). In near-equilibrium regions, where σ is small and spatially smooth, τ is large, and the step size h is automatically increased. Computational efficiency is thereby maximized while thermodynamic consistency is preserved. In far-from-equilibrium regions, where σ is large and rapidly varying, τ decreases, and the step size h is correspondingly reduced to ensure accurate capture of entropy production peaks and detailed energy dissipation behavior. Through real-time feedback of τ, the simulation step size h is nonlinearly and adaptively adjusted. In this manner, the traditional limitation of step-size control detached from physical principles is overcome.

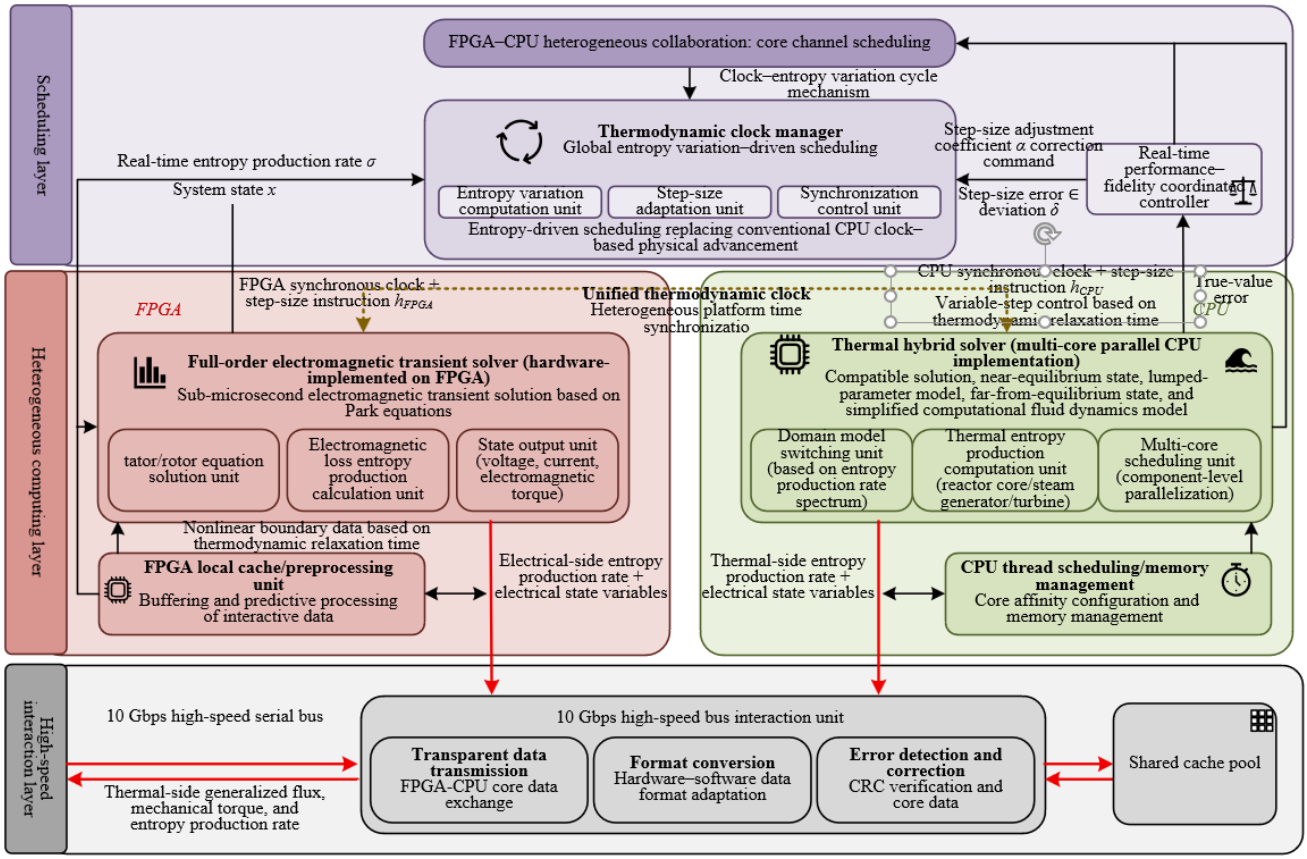

Figure 4. Field-programmable gate array and central processing unit (FPGA–CPU) heterogeneous collaborative real-time solution architecture

An FPGA–CPU heterogeneous collaborative real-time solution architecture is constructed to fully exploit the complementary performance advantages of the two computing platforms, enabling efficient parallel solution of the electrical and thermal subsystems. On the electrical side, the parallel pipelined architecture of the FPGA is utilized to execute full-order electromagnetic transient simulations. A generator electromagnetic transient model is established based on the Park transformation equations, and hardware-level logic implementation enables sub-microsecond solution cycles. In this manner, abrupt entropy production variations induced by electromagnetic losses are captured. On the thermal side, a multi-core CPU parallel architecture is employed to execute a hybrid solution strategy combining a simplified computational fluid dynamics model and lumped-parameter models. The thermal system is partitioned into multiple component-level computational units, and a synchronized parallel solution is achieved through multi-core scheduling. This strategy ensures an effective balance between computational accuracy and efficiency. Data interaction between the heterogeneous platforms is realized through a high-speed communication bus, guaranteeing coordinated solution progress between the electrical and thermal subsystems. The FPGA–CPU heterogeneous collaborative real-time solution architecture is illustrated in Figure 4.

A thermodynamic clock manager governed by global entropy variation is designed to replace traditional CPU clock-cycle-based scheduling logic. Through this mechanism, simulation progression is deeply aligned with thermodynamic evolution. The global entropy variation ΔS is defined as the integral of the system-wide entropy production rate over a single simulation step:

$$\Delta S = \int_{t}^{t+\mathrm{h}} \dot{S}_{gen}\, dt \tag{10}$$

where, $\dot{S}_{gen}$ denotes the global entropy production rate and h represents the current simulation time step. The thermodynamic clock manager computes ΔS in real time. When ΔS reaches a prescribed threshold ΔS_0, subsystem synchronization and boundary data exchange are triggered. If the threshold is not reached, the current step is dynamically extended until the entropy variation constraint is satisfied. By placing thermodynamic evolution at the center of the scheduling logic, the simulation trajectory remains intrinsically consistent with the physical evolution of the system, thereby avoiding the decoupling between simulation time and physical processes that may arise under conventional

CPU-clock-driven scheduling.

A coordinated assurance mechanism for real-time performance and physical fidelity is further established to achieve optimal balance between these two objectives. This mechanism operates through three synergistic layers. Dynamic adaptation between step-size control and thermodynamic relaxation time, ensuring high-resolution simulation under far-from-equilibrium conditions and high computational efficiency in near-equilibrium regions. Heterogeneous task allocation, whereby the FPGA is dedicated to high-frequency electromagnetic transient computation and the CPU to parallel thermal computation, thereby maximizing computational resource utilization. Real-time verification and feedback adjustment, in which step-size suitability and entropy production consistency are continuously monitored. When deviations in real-time performance or thermodynamic consistency are detected, the step-size adjustment coefficient α and heterogeneous scheduling priorities are automatically modified. A real-time error ε and a physical fidelity deviation δ are defined, subject to the constraints $\varepsilon \leq 10$ μs and $\delta \leq 5\%$. Through closed-loop feedback regulation, coordinated optimization of real-time performance and thermodynamic fidelity is achieved. This integrated framework provides robust technical support for real-time simulation of electrical–thermal coupling systems in nuclear power plants.

6. SIMULATION VALIDATION AND RESULTS ANALYSIS

6.1 Validation platform, operating conditions, and evaluation metrics

To validate the effectiveness and superiority of the proposed methodology, an FPGA–CPU heterogeneous collaborative simulation platform was established. Representative operating conditions and quantitative evaluation metrics were defined to provide a unified benchmark for performance assessment. The validation platform was configured with a Xilinx UltraScale+ FPGA (xc7z045ffg900-2) and an Intel Xeon Gold 6248 CPU (24 cores, 48 threads, 2.5 GHz base frequency), equipped with 32 GB DDR4 memory. The simulation software was independently developed using C++ (CPU side) and Verilog (FPGA side). An interface with a data transmission rate of 10 Gbps was employed. Three representative operating scenarios of the high- and medium-voltage electrical–thermal coupling system were selected, encompassing both steady-state and transient disturbance conditions. Four categories of core evaluation metrics were defined to comprehensively quantify thermodynamic consistency, decomposition performance, interaction accuracy, and real-time capability. The detailed platform specifications and operating condition parameters are summarized in Tables 1 and 2.

Table 1. Simulation validation platform parameters

Hardware / Software Type	Specifications
Field-programmable gate array (FPGA) chip	Xilinx UltraScale+ xc7z045ffg900-2; 450,000 logic cells; 220 Digital Signal Processing (DSP) slices
Central processing unit (CPU)	Intel Xeon Gold 6248; 24 cores/48 threads; 2.5 GHz; 35.75 MB cache
Memory	32 GB DDR4; 2933 MHz
Bus transmission	PCIe 4.0; 10 Gbps transfer rate
Simulation software	Independently developed; C++ (CPU side), Verilog (FPGA side); adjustable solver time step
Working fluid property model	Water–steam thermophysical properties based on the International Association for the Properties of Water and Steam Industrial Formulation 1997 (IAPWS-IF97)
Electromagnetic transient model	Generator Park equations; transient step size 0.1 μs

Table 2. Representative simulation operating conditions

Operating Condition	Description	Key Parameter Settings	Simulation Duration
Steady-state operation	Rated-load operation without external disturbance	Rated power 1000 MW; coolant flow rate 4000 t/h; steam pressure 16.7 MPa	100 s
Grid short-circuit condition	Three-phase short circuit at the high-voltage side with post-fault recovery	Fault at t = 20 s; fault duration 0.1 s; recovery at t = 20.1 s	100 s
Steam load sudden change	Secondary-side steam load drop followed by recovery	Load reduced from 100% to 70% at t = 20 s; restored to 100% at t = 40 s	100 s

6.2 Verification of thermodynamic characteristics

The verification of thermodynamic characteristics was conducted to evaluate the thermodynamic consistency of the proposed methodology. Particular emphasis was placed on validating global entropy production non-negativity, entropy wave propagation tracking accuracy, and physical consistency. These indicators collectively ensure that the simulation evolution remains aligned with the fundamental principles of non-equilibrium thermodynamics. The validation results under the three representative operating conditions are summarized in Table 3.

As shown in Table 3, the global entropy production rate remained strictly non-negative under all three operating conditions, and no intervals of negative entropy production were observed. This outcome confirms strict compliance with the second law of thermodynamics and validates the rationale of elevating the second law to a first-principles foundation within the real-time simulation framework. Under steady-state operation, the system remained in a near-equilibrium regime. The global entropy production exhibited minimal fluctuation, and the physical consistency deviation rate was limited to 2.1%. The entropy wave tracking error was 1.2%, indicating strong thermodynamic stability under steady conditions. Under grid short-circuit and steam load sudden-change conditions, the system transitioned into far-from-equilibrium

regimes. Significant surges in global entropy production were observed, with a peak value of 1.562 W/(m³·K). However, entropy wave tracking errors were maintained below 3%, and physical consistency deviation rates did not exceed 3.8%. Furthermore, entropy wave response delays were kept below 1 μs, demonstrating that abrupt entropy production variations and entropy wave propagation induced by disturbances were captured with high temporal precision. These results demonstrate that the proposed methodology effectively preserves thermodynamic consistency throughout the simulation process. The evolution of entropy production was shown to closely match the underlying physical behavior.

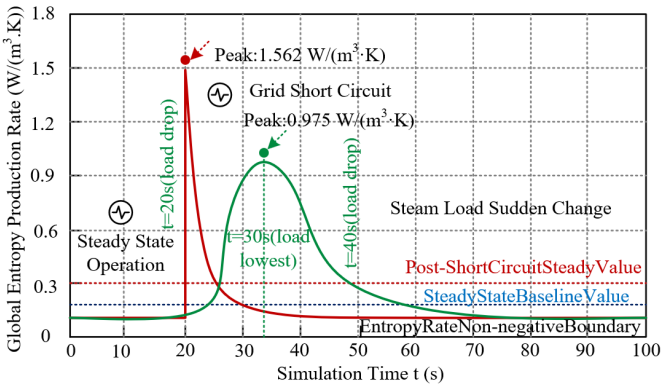

Figure 5. Time response curves of global entropy production under representative operating conditions

To evaluate the capability of the proposed method to capture the dynamic evolution of global entropy production under different thermodynamic states, time-domain simulations were conducted for the three representative operating conditions. The results are illustrated in Figure 5. As shown in the figure, all three operating conditions maintained steady-state operation from 0 to 20 s. During this interval, the global entropy production rate remained stable at approximately 0.084 W/(m³·K) and was strictly non-negative throughout the simulation, satisfying the second law of thermodynamics. This behavior reflects the low-dissipation characteristics of near-equilibrium operation. Under the grid short-circuit condition, a sudden disturbance was introduced at t = 20 s. The global entropy production rate exhibited an instantaneous surge, reaching a peak value of 1.562 W/(m³·K). Subsequently, the entropy production rapidly decreased and stabilized at a level slightly above the initial steady-state value. This response demonstrates the high-dissipation characteristics associated with far-from-equilibrium states under strong electromagnetic disturbances. Under the steam load sudden-change condition, the entropy production rate began to increase progressively at t = 20 s. A peak value of 0.975 W/(m³·K) was observed at approximately t = 30 s, corresponding to the minimum load level. After the load was restored at t = 40 s, the entropy production gradually returned to the initial steady-state level, exhibiting a smoother disturbance response pattern compared with the short-circuit scenario. No negative entropy production intervals were observed in any of the three cases. The entropy production evolution curves accurately characterized thermodynamic dissipation dynamics under varying disturbance intensities. These results confirm that the proposed methodology reliably captures the evolution law of entropy production and achieves a unified representation of numerical stability and thermodynamic stability. The thermodynamic consistency enforced by the framework provides robust support for physics-driven real-time simulation of complex energy systems.

6.3 Validation of dynamic model decomposition performance

The validation of model decomposition performance focused on the effectiveness of dynamic boundary layer adaptive identification and the computational efficiency of domain-partitioned solution. The objective was to evaluate the accuracy and efficiency of the dynamic model decomposition method based on entropy production rate spectrum analysis. The validation results are summarized in Table 4.

Table 3. Thermodynamic characteristic validation results

Operating Condition	Global Entropy Production Range (W/(m³·K))	Entropy Wave Tracking Error (%)	Physical Consistency Deviation (%)	Negative Entropy Production Interval	Entropy Wave Response Delay (μs)
Steady-sate operation	0.082–0.086	1.2	2.1	None	—
Grid short-circuit condition	0.083–1.562	2.7	3.8	None	0.8
Steam load sudden change	0.082–0.975	2.3	3.2	None	0.6

Table 4. Model decomposition performance validation results

Operating Condition	Dynamic Boundary Tracking Accuracy (%)	Domain-Partitioned Solution Time (ms)	Full High-Fidelity Model Time (ms)	Efficiency Ratio (Partitioned/Full)	Boundary Update Frequency (kHz)
Steady-state operation	1.1	18.6	48.2	0.386	10
Grid short-circuit condition	2.4	27.3	49.1	0.556	85
Steam load sudden change	2.0	23.8	48.7	0.489	62

As indicated in Table 4, the dynamic boundary tracking accuracy remained below 2.5% for all three operating conditions, satisfying the predefined evaluation criteria. These results demonstrate that the entropy production rate spectrum–based adaptive identification algorithm accurately captures both the spatial location and temporal evolution of dynamic

boundary layers. Under steady-state operation, the entropy production distribution was spatially smooth, and the boundary update frequency was relatively low (10 kHz). The efficiency ratio of the domain-partitioned solution was 0.386, corresponding to a 61.4% reduction in computational time compared with the full high-fidelity model. This outcome reflects the computational advantage of reduced-order modeling. Under the grid short-circuit condition, entropy wave propagation became intense, and the boundary update frequency increased to 85 kHz to enable real-time tracking of the entropy wavefront. Although the efficiency ratio increased to 0.556, a 44.4% reduction in computational time relative to the full model was still achieved. Under the steam load sudden-change condition, the boundary update frequency reached 62 kHz, and the efficiency ratio was 0.489. This balance indicates that accurate boundary tracking and computational efficiency were simultaneously maintained. Collectively, these results confirm that the proposed dynamic model decomposition method adaptively adjusts partition boundaries and model complexity according to the thermodynamic state of the system. High boundary tracking accuracy is preserved while computational efficiency is significantly enhanced. Consequently, efficient model support is provided for real-time simulation.

To evaluate the capability of the proposed methodology to capture entropy wave propagation and to adaptively update dynamic boundaries under strong disturbances, simulations were conducted for a three-phase grid short-circuit condition. The entropy wave propagation pattern and dynamic boundary trajectory are illustrated in Figure 6. As shown in the figure, the short-circuit disturbance was initiated at the generator location at t = 20 s. Immediately following the disturbance, a high-entropy-production region was generated and propagated in the form of an entropy wave toward the high- and medium-pressure turbine stages and the steam generator. The proposed method captured the entropy wavefront within 0.5 s and completed adaptive updating of the dynamic boundary layer accordingly. Prior to the disturbance, the dynamic boundary remained stable. After the short circuit occurred, the boundary rapidly shifted toward the generator region, where entropy production intensified. The maximum boundary displacement was reached at approximately t = 20.5 s, after which the boundary gradually stabilized. The dynamic boundary trajectory clearly delineated the far-from-equilibrium high-fidelity solution region from the near-equilibrium reduced-order solution region. These results demonstrate that the proposed method is capable of real-time adjustment of partition boundaries along the entropy wave propagation path. Even under strong disturbances, the global entropy production non-negativity constraint was maintained, thereby ensuring unified numerical stability and thermodynamic stability. This provides a rigorous physical foundation and technical support for adaptive domain decomposition in complex coupled systems.

6.4 Validation of data interaction performance

The validation of data interaction performance focused on evaluating the entropy-preserving capability and thermodynamic consistency of the data exchange mechanism based on the maximum entropy production principle. Entropy production deviation and thermodynamic mismatch error during interaction were quantitatively assessed. The validation results are presented in Table 5.

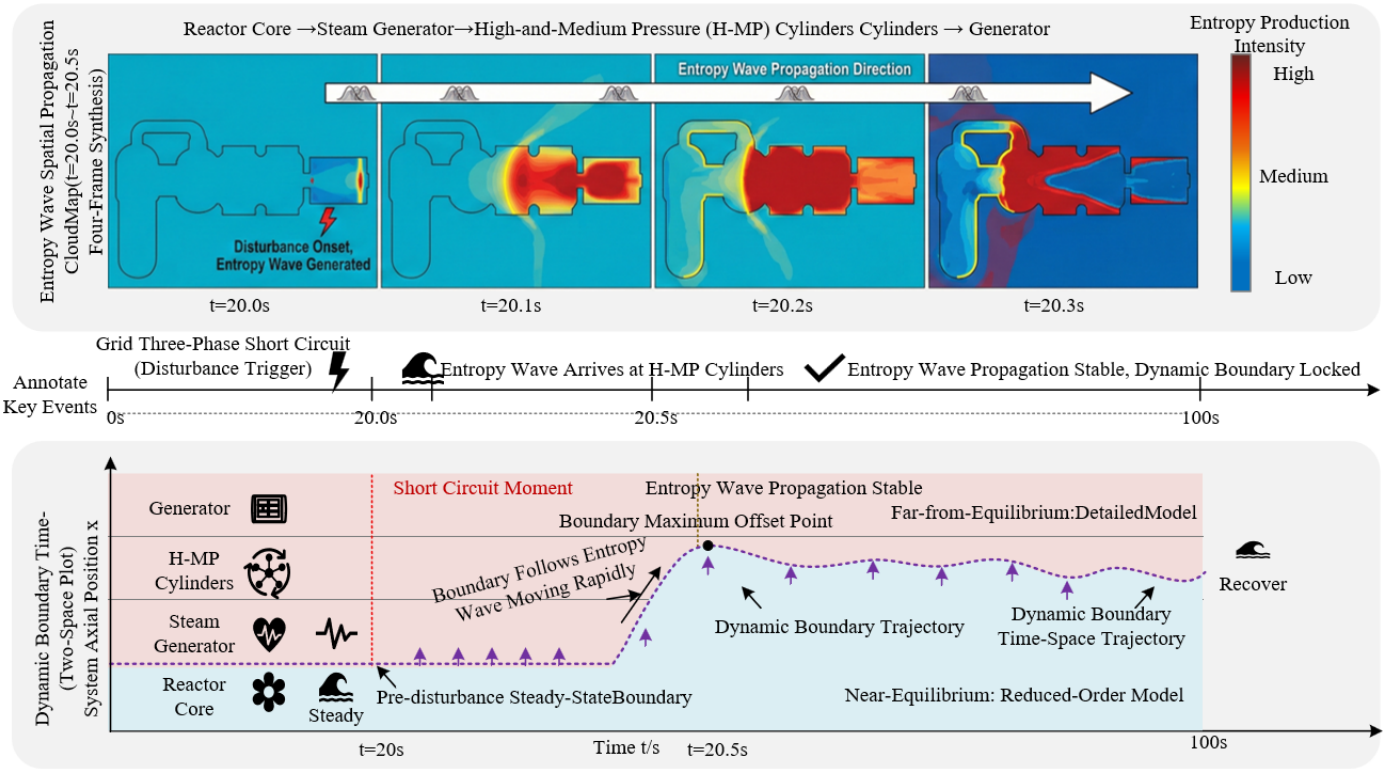

Figure 6. Entropy wave propagation and dynamic boundary trajectory under the grid short-circuit condition

Table 5. Data interaction performance validation results

Operating Condition	Boundary Entropy Production Deviation (%)	Thermodynamic Mismatch Error (W/(m³·K))	Interaction Latency (μs)	Interaction Success Rate (%)	Entropy-Preserving Constraint Satisfaction (%)
Steady-state operation	1.0	0.0003	0.5	100	100
Grid short-circuit condition	1.8	0.0008	0.7	100	100
Steam load sudden change	1.5	0.0006	0.6	100	100

Table 6. Real-time solution performance validation results

Operating Condition	Step-Size Range (μs)	Step-Size Response Delay (μs)	Stiffness-Induced Oscillation Count	Real-Time Compliance Rate (%)	Computational Resource Utilization (%)	Simulation Time/Physical Time Ratio
Steady-state operation	50~100	0.6	0	100	88.2	0.82
Grid short-circuit condition	0.1~20	0.8	1	99.8	92.5	0.98
Steam load sudden change	10~60	0.7	0	99.9	90.3	0.89

As shown in Table 5, the entropy-preserving constraint satisfaction rate and interaction success rate both reached 100% under all three operating conditions. These results indicate that the proposed entropy-preserving data exchange protocol strictly adheres to the maximum entropy production principle and ensures compliant transmission of boundary energy flux and entropy flux. Under steady-state operation, the boundary entropy production deviation was limited to 1.0%, and the thermodynamic mismatch error was as low as 0.0003 W/(m³·K), with an interaction latency of 0.5 μs. These values demonstrate high precision and low latency in interaction. Under the grid short-circuit and steam load sudden-change conditions, significant variations in boundary energy flux and entropy flux occurred due to strong disturbances. Nevertheless, the boundary entropy production deviation remained below 2%, and the thermodynamic mismatch error did not exceed 0.0008 W/(m³·K). Interaction latency was maintained below 0.7 μs. No information loss, artificial energy injection, or violation of entropy balance was observed. These results confirm that the proposed entropy-preserving data interaction mechanism effectively guarantees thermodynamic consistency in cross-domain data exchange. The thermodynamic mismatch issues inherent in conventional interaction methods are fundamentally eliminated, thereby providing robust support for the global stability of the simulation system.

6.5 Validation of real-time solution performance

The validation of real-time solution performance focused on the adaptive capability of the nonlinear variable-step control law, the mitigation of numerical stiffness, and the real-time compliance rate. The objective was to evaluate the effectiveness of the thermodynamic-time-oriented real-time solution strategy. The validation results are summarized in Table 6.

As indicated in Table 6, the proposed nonlinear variable-step solution strategy demonstrates strong adaptive capability and robust real-time performance. Under steady-state operation, the system remained in a near-equilibrium regime. The simulation step size was maintained within 50–100 μs, and the step-size response delay was limited to 0.6 μs. Computational resource utilization reached 88.2%, and the ratio of simulation time to physical time was 0.82, indicating sufficient real-time margin. Under the grid short-circuit condition, pronounced stiffness characteristics emerged. The step size was rapidly reduced to a range of 0.1–20 μs to accurately capture entropy production peaks. Only a single minor numerical oscillation was observed. The real-time compliance rate reached 99.8%, computational resource utilization increased to 92.5%, and the simulation time to physical time ratio was 0.98, satisfying real-time operational requirements. Under the steam load sudden-change condition, the step size was dynamically adjusted within the range of 10–60 μs. No numerical oscillations were detected. The real-time compliance rate reached 99.9%, and computational resource utilization was 90.3%, demonstrating an effective balance between real-time performance and fidelity. These results confirm that the proposed real-time solution strategy dynamically adjusts the simulation step size in accordance with thermodynamic relaxation characteristics. Strong stiffness effects inherent in strongly coupled systems are effectively mitigated, while high real-time compliance rates are consistently maintained. The strategy satisfies the engineering requirements for real-time simulation of electrical–thermal coupling systems in nuclear power plants.

6.6 Comparative analysis with the conventional method

A conventional fixed-step simulation approach based on mathematical stiffness analysis was selected as the benchmark for comparison. Only core performance indicators were evaluated to highlight the advantages of the proposed methodology. The comparative results are summarized in Table 7.

Table 7. Comparison of core performance metrics with the conventional method

Evaluation Metric	Proposed Method (Average)	Conventional Method (Average)	Performance Improvement (%)
Entropy deviation (%)	2.3	12.8	82.0
Numerical robustness (instability events/three conditions)	0	4	100
Computational resource utilization (%)	90.3	65.7	37.4
Real-time compliance rate (%)	99.9	88.5	12.9
Dynamic boundary tracking accuracy (%)	1.8	8.7	79.3
Thermodynamic mismatch error (W/(m³·K))	0.0006	0.0042	85.7

As indicated by the comparative results in Table 7, the proposed methodology outperformed the conventional approach across all core performance metrics. The entropy deviation was reduced to 2.3%, representing an 82.0% improvement relative to the conventional method, thereby demonstrating substantially enhanced thermodynamic fidelity. In terms of numerical robustness, no simulation instability events were observed under the three representative operating conditions, whereas four instability events occurred with the conventional method. This corresponds to a 100% improvement in robustness and confirms that stiffness-induced instability under strong disturbances was effectively eliminated. Computational resource utilization reached 90.3%, reflecting a 37.4% improvement compared with the conventional approach and indicating significantly enhanced computational efficiency. The real-time compliance rate increased to 99.9%, corresponding to a 12.9% improvement and fully satisfying real-time simulation requirements. Dynamic boundary tracking accuracy improved to 1.8%, yielding a 79.3% enhancement in partition precision. Furthermore, the thermodynamic mismatch error was reduced to 0.0006 W/(m³·K), representing an 85.7% decrease relative to the conventional method. This result confirms that thermodynamic inconsistency was fundamentally resolved. Collectively, these comparative results demonstrate that the inherent limitations of traditional simulation paradigms were effectively overcome. Significant improvements were achieved in thermodynamic consistency, numerical robustness, real-time compliance, and computational efficiency, indicating strong engineering applicability and methodological innovation.

When the six categories of validation results are considered comprehensively, it is demonstrated that the proposed model decomposition and real-time simulation framework for high- and medium-voltage electrical–thermal coupling systems in nuclear power plants—constrained by the second law of thermodynamics—strictly satisfies thermodynamic consistency requirements. The global entropy production rate remained non-negative throughout all operating conditions, and high accuracy was achieved in entropy wave propagation tracking and dynamic boundary identification. The dynamic model decomposition method adaptively matched model complexity to the thermodynamic state of the system, thereby significantly improving computational efficiency. The entropy-preserving data interaction mechanism effectively eliminated thermodynamic mismatch, ensuring physical authenticity of cross-domain data exchange. The nonlinear variable-step solution strategy successfully mitigated numerical stiffness and enabled coordinated optimization of real-time performance and physical fidelity. Compared with the conventional method, substantial improvements were consistently observed across all core performance indicators. The effectiveness, superiority, and engineering applicability of the proposed methodology were therefore comprehensively validated, providing a reliable technical framework for high-precision real-time simulation of high- and medium-voltage electrical–thermal coupling systems in nuclear power plants.

7. DISCUSSION

Through deep integration of non-equilibrium thermodynamics and engineering real-time simulation, a paradigm shift in thermodynamics-driven numerical simulation has been achieved. The second law of thermodynamics, traditionally treated merely as a posteriori validation criterion, has been elevated to the status of a first-principles foundation and central organizing logic for real-time simulation of electrical–thermal coupling systems. By constructing a thermodynamically constrained manifold, a unified mathematical representation of numerical stability and thermodynamic stability has been established. The proposed original methodologies—including entropy production rate spectrum analysis, maximum entropy production principle–constrained interaction, and thermodynamic-time-driven variable-step control—systematically extend the application framework of non-equilibrium thermodynamics to the numerical evolution of distributed energy systems. The resulting paradigm is not restricted to a specific system architecture; rather, its fundamental criteria are applicable to a broad class of multiphysics coupled systems characterized by irreversible energy conversion. The universality of the second law of thermodynamics as a foundational physical constraint for simulation has thus been substantiated. Furthermore, a novel theoretical pathway has been opened for interdisciplinary research at the interface of non-equilibrium thermodynamics, computational mechanics, and numerical simulation.

The proposed methodology has been specifically developed to address the multiscale and strongly stiff characteristics of high- and medium-voltage electrical–thermal coupling systems in nuclear power plants. A practically deployable real-time simulation solution has thereby been formed, demonstrating substantial engineering value. The framework can be directly integrated into full-scope nuclear power plant real-time simulation platforms, enhancing both simulation fidelity and numerical robustness under steady-state and transient operating conditions. The method enables accurate reproduction of energy evolution and entropy production distribution under representative disturbance scenarios, such as grid short-circuit events and sudden steam load variations. Reliable thermodynamic data support is thereby provided for fault mechanism inversion and fault localization. In addition, a high-precision real-time validation environment can be established for coordinated control and fault-tolerant control strategies of nuclear generating units. By reducing on-site

commissioning risks and associated costs, the framework offers significant support for safe, stable, and intelligent operation and maintenance of nuclear power plants.

The proposed methodology possesses clearly defined applicability boundaries and inherent limitations. Superior performance is maintained within the high- and medium-voltage sections of nuclear power plants under conventional energy conversion processes spanning near-equilibrium to far-from-equilibrium regimes. However, under extreme transient conditions characterized by intense phase transitions, strong multiphase flow coupling, or highly non-equilibrium shock phenomena, further refinement of local entropy production rate modeling is required. The performance of the framework depends on accurate real-time identification of key thermodynamic parameters and characteristic boundary temperatures of critical components. Measurement or estimation errors in these parameters may influence entropy production rate calculation and dynamic boundary identification accuracy. In addition, the present investigation focuses on electrical–thermal coupling systems in nuclear power plants. For complex multi-energy systems incorporating chemical energy storage, hydrogen energy conversion, and large-scale renewable integration, the entropy production rate models and interaction protocols would require adaptive reconstruction.

Future research will proceed along two principal directions. First, the thermodynamics-driven real-time simulation framework will be extended to multi-energy coupling scenarios, including wind–solar–nuclear–storage hybrid systems and integrated energy systems. In such contexts, entropy production rate formulations and dynamic coupling criteria across multiple energy forms will be reconstructed to enhance cross-scenario applicability. Second, deeper integration between non-equilibrium thermodynamics and digital twin technology will be pursued. Real-time entropy production monitoring and thermodynamic consistency verification will be embedded within the closed-loop evolution logic of digital twins, enabling both physical entities and virtual models to evolve in strict compliance with the second law of thermodynamics. Furthermore, machine learning techniques may be incorporated to enable rapid prediction of entropy production rate spectra and adaptive optimization of dynamic boundaries, thereby further improving the efficiency and precision of real-time simulation for complex coupled systems.

8. CONCLUSION

To address the multiscale characteristics, strong nonlinearity, and severe numerical stiffness inherent in high- and medium-voltage electrical–thermal coupling systems in nuclear power plants, the second law of thermodynamics was elevated from a posteriori validation criterion to the first-principles foundation and central organizing logic of real-time simulation. A comprehensive non-equilibrium-thermodynamics-driven simulation framework was thereby constructed. A dynamic model decomposition method based on entropy production rate spectrum analysis was established, enabling adaptive identification of dynamic boundary layers and domain-partitioned solution of the coupled system. An entropy-preserving cross-domain data interaction mechanism grounded in the maximum entropy production principle was proposed to ensure physically consistent transfer of energy and entropy flux between electrical and thermal subsystems. A nonlinear variable-step solution strategy oriented toward thermodynamic time was developed to achieve precise matching between simulation step size and intrinsic thermodynamic relaxation characteristics. Through this unified formulation, numerical stability and thermodynamic stability were coherently integrated within a single constraint framework. Simulation results demonstrated that the global entropy production non-negativity constraint was strictly satisfied under all representative operating conditions. Significant improvements were observed in dynamic boundary tracking accuracy, entropy-preserving cross-domain interaction, and real-time solution robustness compared with the conventional method. Numerical stiffness and thermodynamic mismatch issues commonly encountered in strongly coupled systems were effectively mitigated. The integration of non-equilibrium thermodynamics with engineering real-time simulation constitutes a methodological advancement that establishes a fundamentally physics-driven paradigm for complex energy system simulation. The framework provides high-precision and high-reliability theoretical and technical support for nuclear power plant safety analysis, fault mechanism reconstruction, and control strategy validation.

REFERENCES

[1] Belyakov, A.V., Gorbachev, A.N., Mikhailov, V.V., Reutov, B.F., Fokin, A.A. (2017). Installations for producing electrospark erosion-and abrasion-resistant coatings on the blades of steam turbines of thermal and nuclear power plants. Surface Engineering and Applied Electrochemistry, 53(3): 274-284. https://doi.org/10.3103/S1068375517030036

[2] Suraci, S.V., Fabiani, D. (2025). Changes in physical-chemical and electrical properties of cross-linked-polyethylene-insulated cable subjected to radio-thermal aging and simulation of loss-of-coolant accident (LOCA). IEEE Electrical Insulation Magazine, 41(5): 6-18. https://doi.org/10.1109/MEI.2025.11230317

[3] Koleva, R., Babunski, D., Zaev, E. (2025). Identification of the conduit water starting time constant in hydropower plants using LSTM and MLP machine learning algorithms. Precision Mechanics and Digital Fabrication, 2(1): 57-66. https://doi.org/10.56578/pmdf020105

[4] Xie, H., Gu, H., Lu, C., Ping, J. (2020). Online simulation of nuclear power plant primary systems. Science and Technology of Nuclear Installations, 2020(1): 8819239. https://doi.org/10.1155/2020/8819239

[5] Gautam, S., Szczublewski, A., Fox, A., Mahmud, S., et al. (2025). Digital real-time simulation and power quality analysis of a hydrogen-generating nuclear-renewable integrated energy system. Energies, 18(4): 937. https://doi.org/10.3390/en18040937

[6] Kee, M.H., Um, K., Jeong, W., Han, J. (2021). Constrained projective dynamics: real-time simulation of deformable objects with energy-momentum conservation. ACM Transactions on Graphics, 40(4): 160. https://doi.org/10.1145/3450626.3459878

[7] Li, B., Zhao, H., Gao, S., Hu, S. (2020). Digital real-time co-simulation platform of refined wind energy conversion system. International Journal of Electrical Power & Energy Systems, 117: 105676.

https://doi.org/10.1016/j.ijepes.2019.105676
[8] Shabbir, N., Ahmadiahangar, R., Rosin, A., Kilter, J., Martins, J. (2024). Development of realtime co-simulation platform harnessing consumer energy flexibility through an aggregator to provide grid support. IEEE Transactions on Consumer Electronics, 70(4): 6641-6652. https://doi.org/10.1109/TCE.2024.3470241
[9] Li, W., Joós, G., Bélanger, J. (2009). Real-time simulation of a wind turbine generator coupled with a battery supercapacitor energy storage system. IEEE Transactions on Industrial Electronics, 57(4): 1137-1145. https://doi.org/10.1109/TIE.2009.2037103
[10] Haldar, S., Bhandari, P., Chakraborty, S. (2017). Emergent Scenario in first and second order non-equilibrium thermodynamics and stability analysis. Annals of Physics, 387: 203-212. https://doi.org/10.1016/j.aop.2017.10.013
[11] Mahmood, D.T. (2025). Thermal transport in porous structures: Mechanisms, modeling approaches, and future directions. Power Engineering and Engineering Thermophysics, 4(1): 42-57. https://doi.org/10.56578/peet040104
[12] Zhong, Z., Fang, J., Hu, K., Li, H., et al. (2026). Real-Time coordination of electrical and thermal energy in power-to-hydrogen by electrolysis plant. Energy Conversion and Management, 347, 120580. https://doi.org/10.1016/j.enconman.2025.120580
[13] Marco, J., Kumari, N., Widanage, W.D., Jones, P. (2015). A cell-in-the-loop approach to systems modelling and simulation of energy storage systems. Energies, 8(8): 8244-8262. https://doi.org/10.3390/en8088244
[14] Rizal, R.F., Munir, M. (2024). Enhancing the sustainability of PVT systems through optimized PCM selection and container configuration: A CFD approach. Power Engineering and Engineering Thermophysics, 3(4): 266-278. https://doi.org/10.56578/peet030404
[15] Comodi, G., Giantomassi, A., Severini, M., Squartini, S., et al. (2015). Multi-apartment residential microgrid with electrical and thermal storage devices: Experimental analysis and simulation of energy management strategies. Applied Energy, 137: 854-866. https://doi.org/10.1016/j.apenergy.2014.07.068
[16] Jia, Y., Han, P., Shi, Z., Zhang, L. (2025). Interface-based parallel and multi-rate real-time simulations for thermal-electric systems. Engineering Reports, 7(5): e70175. https://doi.org/10.1002/eng2.70175
[17] Cheong, P.C.K., Foucart, F., Duez, M.D., Offermans, A., Muhammed, N., Chawhan, P. (2024). Energy-dependent and energy-integrated two-moment general-relativistic neutrino transport simulations of a hypermassive neutron star. The Astrophysical Journal, 975(1): 116. https://doi.org/10.3847/1538-4357/ad7825
[18] Dahlburg, J., Corones, J., Batchelor, D., Bramley, R., et al. (2001). Fusion simulation project: integrated simulation and optimization of magnetic fusion systems. Journal of Fusion Energy, 20(4): 135-196. https://doi.org/10.1023/A:1023433001854
[19] Hoth, K., Steffen, T., Wiegel, B., Youssfi, A., et al. (2021). Holistic simulation approach for optimal operation of smart integrated energy systems under consideration of resilience, economics and sustainability. Infrastructures, 6(11): 150. https://doi.org/10.3390/infrastructures6110150
[20] Malkawi, A., Yan, B., Chen, Y., Tong, Z. (2016). Predicting thermal and energy performance of mixed-mode ventilation using an integrated simulation approach. Building Simulation, 9(3): 335-346. https://doi.org/10.1007/s12273-016-0271-x
[21] Bornman, W., Dirker, J., Arndt, D.C., Meyer, J.P. (2017). Integrated energy simulation of a deep level mine cooling system through a combination of forward and first-principle models applied to system-side parameters. Applied Thermal Engineering, 123: 1166-1180. https://doi.org/10.1016/j.applthermaleng.2017.05.163